M.A. Camerucci*, A.L. Cavalieri*, P.G. Galliano**, A.G. Tomba Martinez*

Chemical Wear of Commercial Magnesia-Carbon Refractory Bricks in Air

THE AUTHOR

The corresponding author, **Dr. A.G. Tomba Martinez**, studied Materials Science at the Mar del Plata University (Argentina), where she earned her PhD in 1998. From 2008, she leads a research group (together with Dr. M.A. Camerucci) dedicated to study the processing and the mechanical behaviour of structural ceramics. Besides the academic research, the group has maintained a strong relationship with the local steelmaking industry since 1998, working in several aspects of refractory materials, including both mechanical behaviour and corrosion wear. Since 2001, Dr. Tomba Martinez has been part of the teaching staff of Engineering Faculty of the Mar del Plata University, and since 2002 she has been working as a researcher at the Materials Science and Technology Research Institute (INTEMA) that belongs to the Research National Council of Science and Technical Researches (CONICET, Argentina).
E-Mail: agtomba@fi.mdp.edu.ar

ABSTRACT

In this work, the chemical degradation in air of different commercial MgO-C refractories used in the steelmaking industry was studied. Materials were characterized by mineralogical, microstructural, differential thermal and thermo-gravimetric analyses and measurements of density and porosity. Cylindrical samples were subjected to isothermal treatments at different temperatures and times in air and then, the weight loss and percentage of decarburized area were determined. Moreover, different surface conditionings (protective antioxidant paint and graphite powder muffle) were evaluated in regard to gas attack, and compared with non-conditioned specimens. The obtained results showed differences between the studied refractory materials according to the experimental conditions (temperature and time). At the low temperature regimen, pitch-based refractories exhibited the smallest chemical degradation whereas at high temperature, the material bonded with resin was the most resistant to oxygen chemical attack. The analysis of other phenomena related to microstructural changes helps to achieve a description of thermo-chemical processes occurring in the refractory samples during thermal treatments.

KEYWORDS

MgO-C refractories, binder pyrolysis, direct oxidation, indirect oxidation

Interceram 61 (2012) [4]

1 Introduction

Chemical wear of MgO-C refractories in liquid and gaseous environments is a critical issue that strongly affects the performance of lining materials in the steelmaking industry. In particular, direct oxidation of graphite by air (reaction I) at the hot face of the bricks becomes critical above 700 °C and alters the porosity, the slag corrosion resistance, and the mechanical performance of the refractory lining.

$$2C(s) + O_2(g) \leftrightarrow 2CO(g) \qquad (I)$$

According to the study of Li et al. [1], the only product of graphite oxidation at temperatures higher than 1000 °C is $CO_2(g)$ formed by the combination of CO(g) and O_2 at a temperature <900 °C. Air oxidation of graphite in oxide-C lining refractories may occur during different stages of the steelmaking process such as tapping, vessel preheating, and hot repairing, among others [2–3].

At higher temperatures, the indirect oxidation by reaction II (also known as carbothermal reduction of MgO) contributes to the sealing of pores by recrystallization of MgO in the outer layers (dense zone formation) producing enhanced chemical and mechanical properties of the brick.

$$MgO(s) + C(s) \leftrightarrow Mg(g) + CO(g) \qquad (II)$$

The re-oxidation of magnesium requires the presence of oxygen, CO, or CO_2 [4]. Although reaction (I) is thermodynamically and kinetically favored at temperatures higher than 1400 °C (and low oxygen partial pressure), the presence of metallic antioxidant additives such as Al, Si, Mg or alloys in the brick composition lowers the formation temperature of Mg(g) and/or increases its partial pressure by metallic vaporization and metallothermic reduction [4–5], with beneficial effects on the magnesia recrystallization. Surface dense zones enriched in recrystallized MgO have been observed, mainly in laboratory tests rather than in post-mortem samples [4, 6].

The oxidation of MgO-C materials has been extensively studied including the formulation of reaction mechanisms based on experimental results and thermodynamic and kinetic data. Oxygen from air has been frequently reported as the main oxidant reactant. However, most of these studies are restricted to laboratory-prepared samples, often using precarbonized samples to pyrolyze the organic binder, and a relatively narrow range of temperature or partial pressure of oxygen [1]. The high temperature range has had more attention [1–4, 7–17] in agreement with the conditions prevailing in service (around 1400 °C under conditions of high oxygen availability [6]). Nevertheless, the practices in plants cover a wide range of temperature, from room temperature to 1700 °C and there is also a broad temperature distribution between the hot and the cold faces of the brick. Moreover, in-plant chemical and microstructural changes in MgO-C bricks begin at temperatures around 300 °C (in particular in the organic binder); for these reasons, chemical degradation also has to be evaluated in the low and the mid ranges of temperature. However, there is a small number of works covering the temperature range below 1000 °C [2, 3, 9, 11, 12, 15] where binder reactions occur.

Conversely, works focused on kinetic issues are mainly restricted to MgO-C materials without antioxidant additives [1–3, 9, 10, 13, 14] and only a few of them deal with materials containing Al [16]. Moreover, reports

* Instituto de Investigaciones en Ciencia y Tecnología de Materiales (INTEMA), UNMdP-CONICET, Av. J.B. Justo 4302, (7600) Mar del Plata, Argentina
** Tenaris Siderca R&D (REDE AR), Dr. Simini 250, (2804) Campana, Argentina

on the oxidation resistance of as-received (without precarbonization) commercial materials are not so common [11, 15]. In spite of difficulties associated with the lack of control on composition and the variability associated with commercial bricks, this approach has the advantage of determining the actual properties of the material to be used in the plant and allows more reliable extrapolation to service conditions. Even with a careful selection of materials, some general principles or guidelines for design and use may be obtained.

The chemical resistance of MgO-C refractories to oxidant atmospheres depends on their composition, microstructure, and texture (porosity, quality and mean size of MgO particles, quality and content of graphite and antioxidant additives, and binder type) besides the composition of the gaseous phase and the temperature. In this work, the thermochemical degradation of as-received commercial MgO-C refractories in air is evaluated at 660 and 1400 °C by weight loss determination and measurements of decarburized area. Pitch and resin-bonded bricks containing different metallic additives were compared. The main factors governing the behavior of the bricks were discussed.

2 Experimental

2.1 Materials

Three types of MgO-C commercial bricks (fabricated by the same manufacturer) used in the steelmaking industry for ladle and electric furnace linings were evaluated. They were labeled A1, A2, and B. According to technical data sheets these materials have two different carbon binders: pitch (materials A1 and A2) and resin (material B). They also present different contents of sinter (S) and electrofused (EF) MgO aggregates, as shown in Table 1.

The as-received bricks were characterized by several techniques. Powder samples representative of the whole refractory bricks were prepared by crushing, quartering, and grinding. The mineralogical analysis was carried out on powdered samples (<70 mesh) by X-ray diffraction (XRD; Philips) using Co-K_α radiation at 40 kV and 30 mA with a Ni filter. The Rietveld method was employed for quantitative analysis (FullProf software). The bulk density (ρ_b) and the apparent porosity (π_a) were determined based on the DIN EN 993-1(DIN 51056) standard [18]. The pycnometric density (ρ_{pyc}) was measured on powdered samples (<70 mesh) employing kerosene in accordance with an internal method based on the ASTM C329-88 standard [19]. The true porosity (π_t) and the closed porosity (π_c) were obtained by calculation using the following relationships: $\pi_t = (1 - \rho_b/\rho_{pyc}) \times 100$ and $\pi_c = \pi_t - \pi_a$. The thermal differential (DTA; Shimadzu DTA-50) and thermogravimetric (TGA; Shimadzu TGA-50) analyses were performed on representative powdered samples (<70 mesh) up to 1400 °C (10 °C/min) under flowing air. From TGA data, the amounts of the organic binder and graphite were estimated. The microstructure of bricks was observed by scanning electron microscopy (SEM; Philips XL30) coupled with elementary analysis using an EDAX X-ray (energy dispersion spectroscopy, EDS) detecting unit and reflected light microscopy (RL; Nikon Labophot2-Pol with Optronics 3CCD video system model DEI 750) coupled with a cathodoluminescence accessory (CL; Cambridge Image Technology Ltd. model 8200 Mk3). The surfaces for observation were obtained by transversal cut of cylinders previously stuffed in resin to avoid crumbling of the specimen, and polishing with SiC papers (320 grit) using kerosene as lubricant/coolant.

2.2 Testing

Cylinders of 27.10 ±0.05 mm in diameter and 25.00 ±0.05 mm in length were drilled from bricks (using a diamond drill and a diamond cutting disk). Besides cylinders without surface conditioning (NC specimens), specimens with two different surface conditionings were tested: a) coated with commercial antioxidant paint (P specimens) and b) muffled with graphite powder (M specimens). At first, these surface conditionings were tested as procedures to minimize chemical attack by the oxidant atmosphere in other laboratory tests (for instance, mechanical testing at high temperature [20]). The coating was performed using vacuum impregnation (repeated twice) of an aqueous suspension of a commercial Al_2O_3-based powder. In the muffled condition, a homogeneous thickness of compacted powder (<20 mesh) covered the entire sample and the excess of graphite was verified at the end of the thermal treatments.

Isothermal treatments were performed at 660 °C and 1400 °C, respectively, using a chamber electric furnace with SiC heater elements (10.5 °C/min mean heating rate). The specimens were maintained at each temperature for 3 h or 5 h and free cooled in the furnace chamber. The testing was carried out under an air atmosphere (natural convection).

The temperatures for the treatments covered the low and high regime, and their choice was based on DTA/TGA thermograms. The low temperature (660 °C) was selected with the aim of pyrolyzing the organic binder separately, as much as possible, of the oxidation of graphite and other reac-

Table 1 • Characterization of as-received MgO-C refractories

	Sample A1		Sample A2		Sample B	
S-EF[1]	0.75–0.25		0.25–0.75		0.10–0.90	
Main phases	MgO (Periclase): 92 mass-% C (Graphite): 5–6 mass-%		MgO (Periclase): 93–94 mass-% C (Graphite): 4–5 mass-%		MgO (Periclase): 93–94 mass-% C (Graphite): 6–7 mass-%	
Minor phases	Al: 2–3 mass-%		Al: 2–3 mass-%		Al-Mg, Si: 3–4 mass-%	
ρ_b / g/cm³	3.00 ±0.01		3.00 ±0.01		2.98 ±0.01	
ρ_{pyc} / g/cm³	3.15 ±0.02		3.18 ±0.03		3.17 ±0.04	
π_a / %	3.9 ±0.2		4.6 ±0.1		3.5 ±0.1	
π_t / %	4.8 ±0.2		5.7 ±0.2		5.8 ±0.3	
π_c / %	0.9 ±0.2		1.1 ±0.2		2.3 ±0.3	
T_{peak}^{DTA} / °C[2]	530 610	932	530 610	938	392	890
Δm^{TGA} / mass-%[3]	4.8	8.2	4.2	7.8	2.0	10.0

1) S-EF: Proportions of sintered magnesia (S) and electrofused magnesia (EF) particles estimated from microscopic analysis.
2) T_{peak}^{DTA}: Temperature of the maximum of exothermic peaks in DTA that coincides with mass losses in TGA thermograms.
3) Δm^{TGA}: Mass losses associated with DTA exothermic peaks.

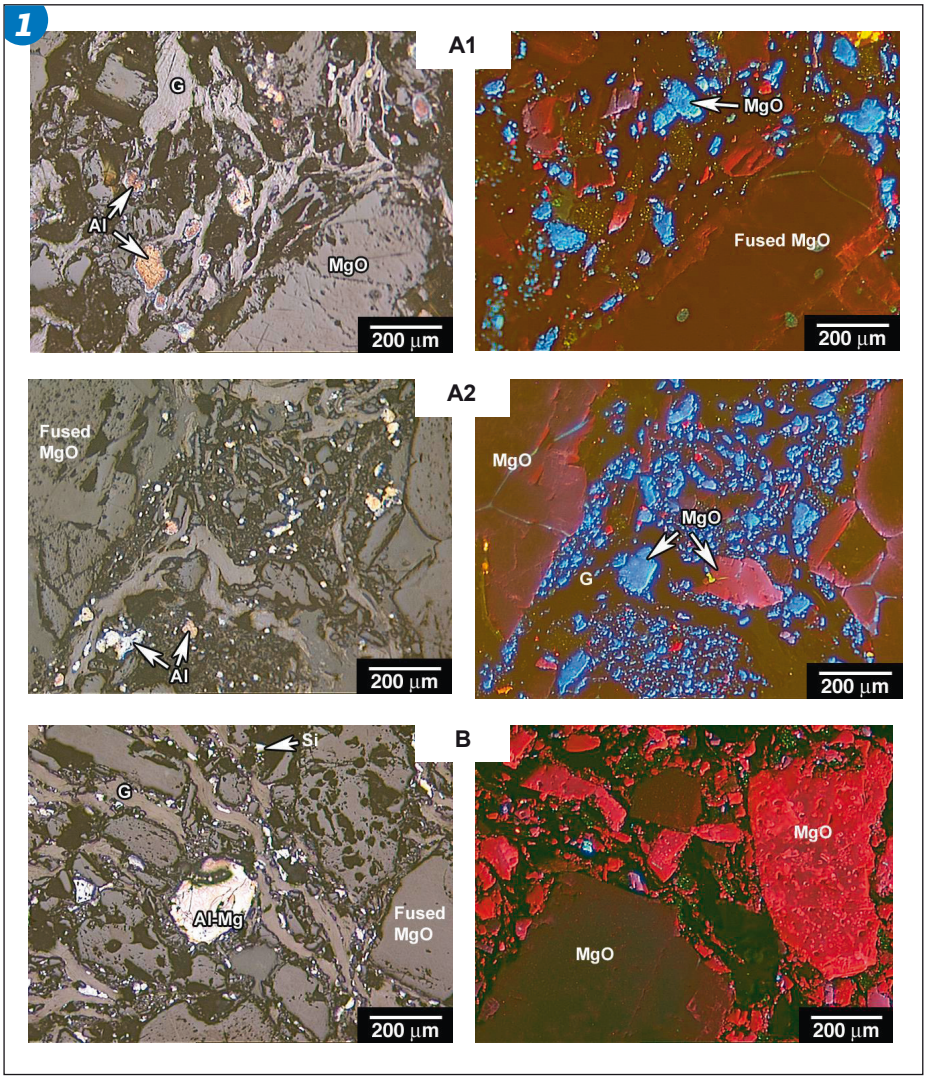

Fig. 1 • CL microscopy images of as-received MgO-C refractories

tions involving the metallic additives during the thermal treatment. The highest temperature, 1400 °C, is commonly used to test this type of material [6] and it was expected that the main reactions between the other inorganic components (oxidation of graphite, reactions of the metallic additives, carbothermal reduction) would occur or were prone to occur under this condition.

After the thermal treatments, the weight loss (±0.001 g) and the decarburized area of the specimen were determined. This last parameter was estimated by image analysis (Image Pro Plus and Adobe Photoshop) of ground surfaces obtained by cross cutting of the cylinders (previously stuffed in polyester resin in vacuum). The digital images were obtained using a stereomicroscope (Zeiss, up to 150×).

As complementary data, the apparent porosity of NC specimens thermally treated over 5 h was determined by the same method used for the as-received refractories. Moreover, the mineralogical analysis of some tested specimens was performed by XRD (Philips) on powder samples (<70 mesh), using Co-K_α radiation (40 kV and 30 mA), with a Ni filter. Conversely, the size distribution of magnesia particles (>0.1 mm) after thermal treatments of NC specimens was also determined from image analysis (Image Pro Plus and Adobe Photoshop) performed on the same polished cross surfaces of tested cylinders used to determine the percentage of decarburized area. The size of each particle was taken as the mean diameter calculated from its area. In every case, the size distribution of MgO particles was determined separately in the inner central zone (dark region when decarburization was observed) and in the outer region (decarburized region) of the cylinders.

3 Results and discussion

3.1 Characterization of the refractory materials

Table 1 shows some of the results obtained from the different characterization techniques used for the as-received refractories.

MgO as periclase and C as graphite were determined as the main crystalline phases in every material, in addition to small amounts of metallic Al; the content of aluminum in A1 and A2 was very similar. The presence of Si as a metallic additive was also identified in material B; considering the experimental error of the Rietveld method (±5 mass-%) and the microstructural analysis, the content of this metal (≈1 mass-%) was lower than the aluminum additive (2–3 mass-%).

The microstructural evaluation of A1, A2, and B samples by SEM/EDS confirmed the results of XRD analysis and the information of technical data sheets. Electrofused and sintered magnesia aggregates were observed in the three refractories, together with small Al particles and graphite flakes (G). The relative amount of EF and S magnesia particles (EF-S) estimated from the microscopic analysis is reported in Table 1. The images obtained by RL/CL observation (Fig. 1) showed additional information such as the presence of Al-Mg alloy (instead of pure Al) in the B material. The sintered MgO was mainly identified in the fine and medium fraction of MgO particles in A1 and A2 refractories whereas higher amounts of electrofused MgO aggregates were confirmed in the resin-bonded refractory (B).

No significant differences were determined between bulk and pycnometric densities of the three refractories, because of similarities in their mineralogical composition. Differences between 10 and 30 % were obtained in open and true porosities of the different bricks (except the values of π_t for A2 and B which were very similar). The highest volume fraction of closed porosity was determined in the B refractory in agreement with the lowest bulk density; however, this material also has the lowest π_a.

Comparing DTA and TGA plots for each refractory (Fig. 2), there are peaks in the former that coincide with weight losses displayed in TGA thermograms. The temperature of the maximum of these peaks (exothermic peaks) determined by DTA and the mass variations by TGA associated with them are reported in Table 1 as T_{peak}^{DTA} and Δm^{TGA}, respectively.

DTA/TGA graphics of pitch-bonded materials A1 and A2 were very similar in position (temperature) and intensity of peaks. DTA peaks and weight losses at temperatures below 650 °C were attributed to the pitch transformations [21], including the mesophase formation, the transformation to semi-coke, and the oxidation of the residual carbon (exothermic peak ≈600 °C). A small endothermic peak around 660 °C due to the melting of the aluminum particles was also displayed in both DTA thermograms. The weight loss displayed at a temperature slightly higher than 930 °C was assigned to

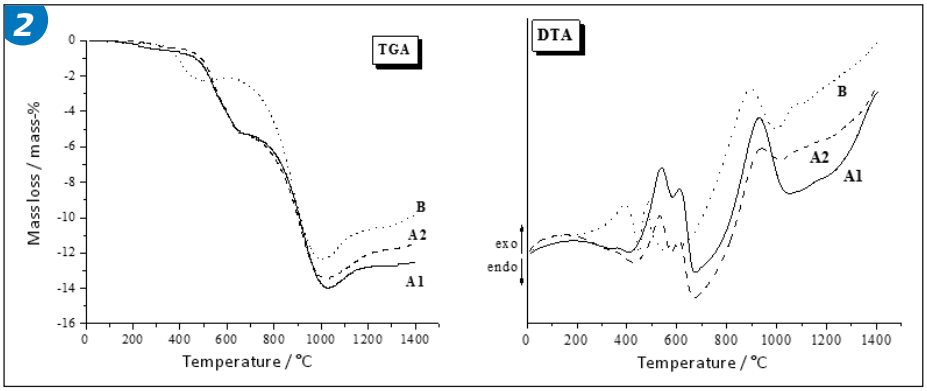

Fig. 2 • TGA and DTA thermograms of as-received MgO-C refractories

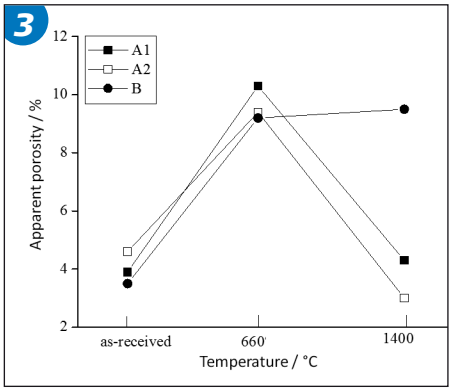

Fig. 3 • Apparent porosity of NC thermally treated specimens (air, 5 h)

the graphite oxidation. At temperatures over 1000 °C, DTA peaks with low definition were identified which could be attributed to the several reactions that occur at this high temperature range involving liquid or gaseous Al and the formation of Al_4C_3, Al_2O_3, and MgO-Al_2O_3 spinel [5, 6, 21, 22].

Compared with pitch-based refractories, different peaks were displayed in DTA/TGA plots of the B material. DTA peaks below 600 °C were attributed to the resin transformations [21, 24, 25] (condensation, oxidation, dehydration, and decomposition reactions), including the oxidation of the residual glassy carbon (exothermic peak ≈580 °C). As reported in the literature [9, 25], the weight losses occurred at lower temperatures in resin-based material than in pitch-containing ones. A very small endothermic peak ≈657 °C was attributed to the melting of Al-Mg alloy. The mass loss displayed at 890 °C (DTA exothermic peak) was assigned to graphite oxidation. At higher temperatures, low-intensity DTA peaks were observed and attributed to the same reactions mentioned above for pitch-bonded materials. Moreover, the reactions of silicon with O_2 (SiO_2 formation and further transformation to SiC) also have to be taken into account [5, 22].

On the basis of the similarity between DTA thermograms of A1 and A2, it could be assumed that the pitch and the graphite flakes have similar qualities for both of them. Since TGA steps (Fig. 2) corresponding to the transformation of the binders (evolution of gases and the oxidation of residual carbon) and to the graphite oxidation were separated in every material (as has been previously reported in TGA performed under an oxidant atmosphere [12, 23]), the content of both components can be estimated from Δm^{TGA} values (Table 1) at temperatures lower than 650 °C and around 900 °C, respectively. Therefore, the contents of the organic binder and the graphite were slightly higher in A1 (4.8 and 8.2 mass-%, respectively) than in A2 (4.2 and 7.8 mass-%, respectively). The difference with the values obtained by quantitative XRD analysis was attributed to the Rietveld method error (±5 mass-%) together with the incidence of the flakes orientation on the intensity of the diffraction peaks. Conversely, the content of the organic binder estimated from the TGA analysis is lower in the B refractory (2 mass-%) and the amount of graphite is higher (10 mass-%) than in pitch-based materials.

As mentioned above (Section 2.2), the selection of the temperature for thermal treatments was performed using DTA/TGA data. As can be observed in Fig. 2, no DTA peaks corresponding to organic binder transformation (including the oxidation of the residual carbon) occurred above 660 °C in any of the materials, and the peak assignable to oxidation of graphite began around this temperature. Similarly, this temperature limited those steps corresponding to the loss of material coming from the organic binder loss (gaseous products and residual carbon) and the graphite loss in TGA thermograms. For this reason, the thermal treatment in the low temperature regime was performed at 660 °C.

3.2 Air tests

The apparent porosity of NC specimens thermally treated over 5 h in air is plotted in Fig. 3. The volumetric fraction of open pores increased after the treatment at 660 °C due to the reactions involving the organic binders (alteration of open and closed pores and cracks due to volatile elimination and volumetric shrinkage [21, 24]). The change in the apparent porosity was similar for the three refractories in spite of the significant differences in the amount of binder in as-received materials (Table 1), which was attributed to the higher volume contraction inherent to the resin binder in respect of the pitch binder as reported in the literature [24].

At higher temperatures (1400 °C), other processes such as the oxidation of graphite, the reduction of oxide impurities [26], Al_4C_3 and spinel formation [26], and reduction of MgO to gaseous Mg (by metallic vaporization and metallothermic or carbothermal reduction) can also be accompanied by the generation of porosity. However, if the formed phases crystallize into open pores or sintering of fine particles occurs [27], the porosity decreases. The complex balance of all these processes determines the apparent porosity at 1400 °C: comparing with the values at 660 °C, the porosity of NC specimens remained almost the same for B whereas a significant reduction of π_a was determined in both pitch-based specimens. After the treatment at 1400 °C, the resin-based refractory was even more porous than A1 and A2. Brandt and Rand [28] showed that the apparent porosity of resin-based MgO-C materials with Al or Si as antioxidants increased from 600 to 1400 °C (in a CO/N_2 atmosphere, 3 h), the increase being more pronounced when aluminum is used (up to around 30 % and 50 % for Si and Al content near 3 mass-%, respectively). Taking into account these results, the sintering of fine particles of MgO and/or the filling of pores should be important contributions to the elimination of pores in the matrix when A1, A2, and B were heated at 1400 °C for 5 h in air.

As examples, Fig. 4 shows transversal views of A1 specimens without conditioning (NC) after different treatments in air. Fig. 5 plots the mass loss and the decarburized area of the three materials thermally treated in air. No decarburized area was visually detected in the specimens treated at 660 °C at any time (3 h or 5 h). The protection with alumina paint reduced the material degradation (around 15–25 % in area and 8–20 % in mass loss) as graphite muffle did, even in a much effective way.

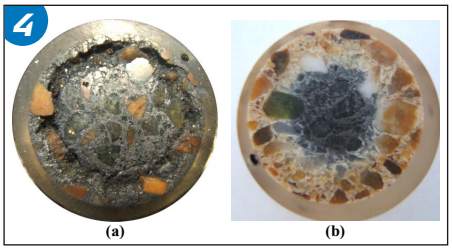

Fig. 4 • NC specimens of A1 after the following thermal treatments (air, 3 h); a) 660 °C, b) 1400 °C

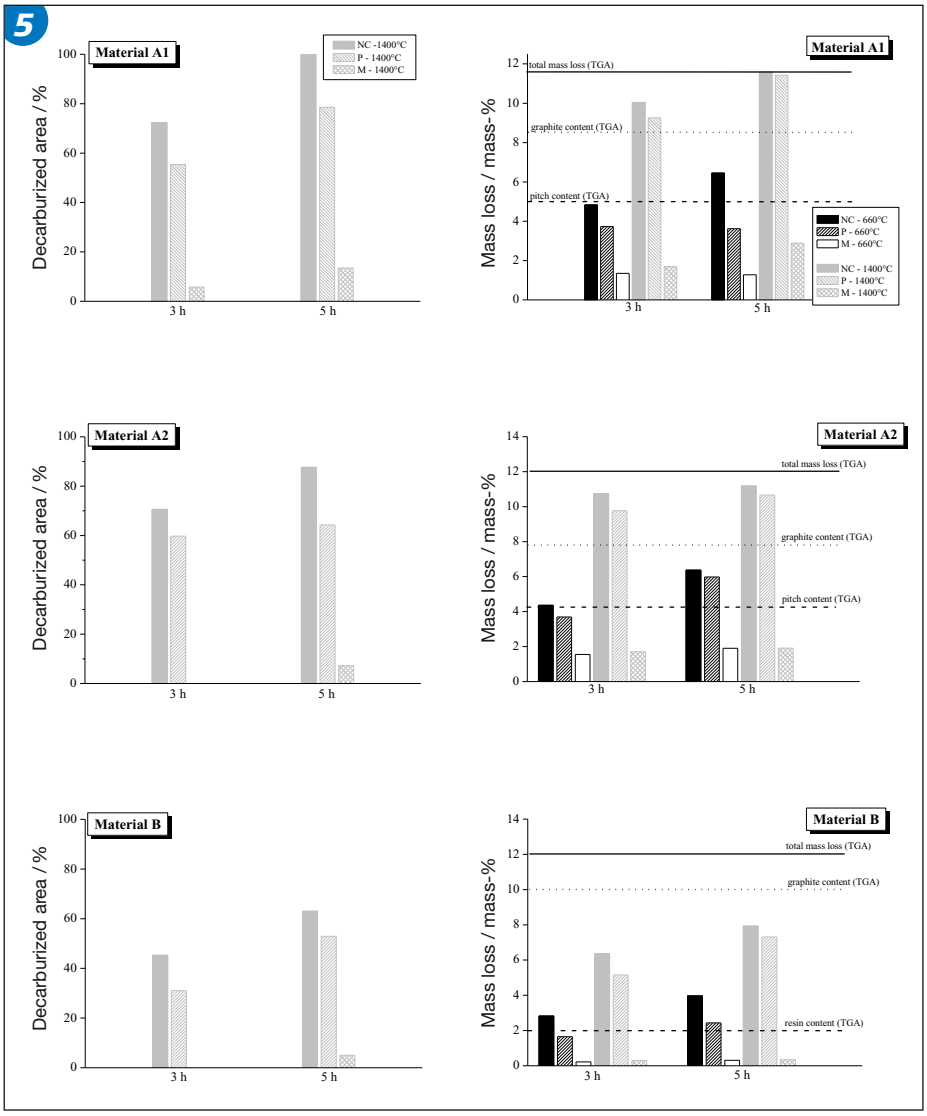

Fig. 5 • Mass losses and decarburized areas of thermally treated specimens of MgO-C refractories (air)

The three materials exhibited similar patterns of mass losses and decarburized areas in respect to the different treatments (surface conditioning, temperature, and time). At 660 °C, the weight loss is mainly due to the pyrolysis of organic binders which is accompanied by the evolution of volatiles and porosity increase. No decarburized area was detected and no significant oxidation of graphite was expected to occur. Except for A1, the binder was completely transformed after 3 h in NC specimens. In addition, the weight loss of B is higher than the binder content (2.8 mass-%) which is attributed to some contribution of graphite oxidation. The TGA thermogram of the B refractory shows that the weight loss due to the reaction of graphite began at a temperature slightly lower than 660 °C (around 630 °C) whereas for the pitch-based refractories, this process began at ≈700 °C. Moreover, the range of temperatures where the phenolic resin pyrolyzed (Fig. 3) was lower than that corresponding to the pitch binder; this fact could also promote a higher advance of transformation of resin in the B material in regard to the other two refractories. The difference between the mass loss of NC specimens of A1 and A2 treated at 660 °C for 3 h is attributed to the higher apparent porosity of the latter (≈18 %). Even when the carbonization is thermally activated, the partial pressure of oxygen also accelerates the process [21]. As the open porosity increases, the amount of oxygen and the pyrolysis advance at any time also increase; this is the reason why A2 lost a larger mass than A1. The decrease of the catalytic effect of O_2 is the reason why the pyrolysis of the binder was slower and the weight losses were smaller in P specimens and even less in M specimens.

After 5 h at 660 °C, the weight losses of NC specimens exceeded the mass loss expected on the basis of the organic binder content in every material which also occurred in P specimens of A2 and B. Even if there was at that point no visual detection of decarburization it is considered that the oxidation of graphite indeed occurred, favored by oxygen partial pressure increasing due to the increase of the open pores volume fraction (Fig. 3).

A ring of detached material was identified in the case of NC and P specimens treated at 660 °C, as is shown in Fig. 4 a. A similar microstructural degradation was already noticed by Takeuchi et al. [12] in oxidation tests of laboratory samples prepared with Al, Si, and B_4C additives. As the exposure time increased, the mean radius of the ring (measured from the cylinder center) decreased; moreover, the ring radius of NC cylinders was always greater than the radius of P specimens at the same time (Fig. 6). This phenomenon is related to the binder transformation, as this is the main process occurring at the low range of temperature; moreover, it is related to the different state of the reaction between the surface and the inside of the specimens. From the beginning of the reaction, different volatile species evolve with the consequent generation of pores and volume shrinkage which produces cracks. During this process, the residual carbon organizes into a solid structure more or less similar to graphite, depending on the type of binder (pitch or resin) [21] leading to a recovery of material cohesion. The concentric advance of the pull out is attributed to the catalytic effect of O_2 on the carbonization of the binder; the oxygen advances more and more into the specimen as pores and cracks are formed. Thus, the oxygen concentration gradient is affected by its superficial partial pressure (lower in P than in NC specimens) and by the evolution of the apparent porosity in the outer layers of the specimen which is also a function of the state of the organic binder transformation. One cannot ignore the small effect on the concentric advance of this microstructural degradation of the thermal gradient and the opposite flow of the gases evolved from the pyrolysis into the cylindrical specimen.

At 1400 °C, after the complete transformation of organic binders (carbonization and oxidation of the residual carbon), the oxidation of graphite occurred in the range 700–900 °C and the metallic additives reacted above 1000 °C. Material A1 without surface

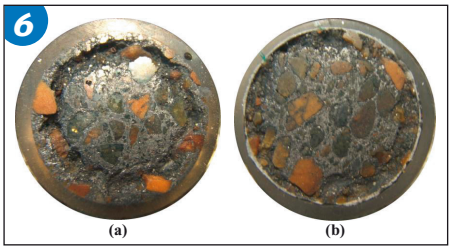

Fig. 6 • Specimens of A1 after the thermal treatments at 660 °C, 3 h (air): a) NC, b) P

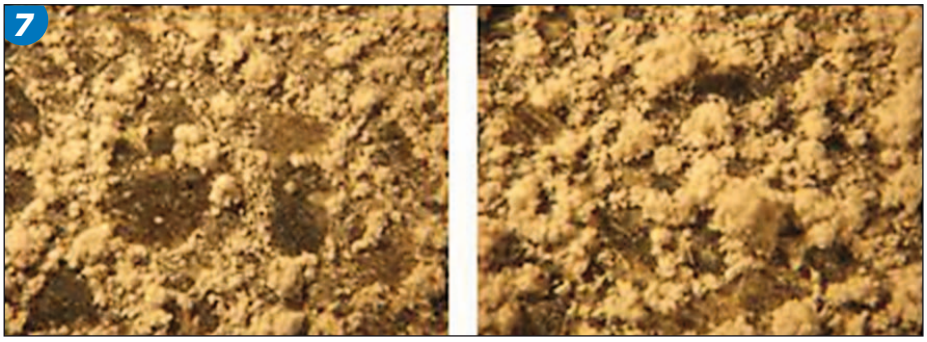

Fig. 7 • MgO powder on the surface of the B specimen without conditioning (NC) treated in air at 1400 °C, 5 h

Fig. 8 Semidecarburized area of the B specimen (NC) tested at 1400 °C (air, 5 h)

conditioning showed completely decarburized surfaces (after 5 h). However, the mass loss did not reach the total carbon mass determined by TGA on powder samples (Fig. 5). This difference between the thermochemical degradation advance measured by the decarburized area and the mass loss is due to: a) errors associated with the experimental measurement of the decarburized area, b) the occurrence of reactions involving the metallic additives which lead to weight increase, and c) the formation of gaseous Mg which could be irreversibly lost. The use of optical inspection for the delimitation of the boundary between the external decarburized area and the inner unreacted zone has uncertainty. Moreover, a decarburized region could still have some unreacted graphite and some graphite could also be oxidized into an apparent unreacted dark zone (as in the case of NC specimens treated at 660 °C for 5 h, for instance).

The reactions involving antioxidants at temperatures above 1000 °C are those mentioned in the discussion of DTA/TGA data of the as-received material which can occur by several mechanisms [5, 6, 21, 22]. Conversely, the formation of Mg (g) begins at temperatures near 1000 °C when Al (950 °C), Si (1100 °C), or Mg-Al (750 °C) are present [4, 5] and gaseous magnesium could be re-oxidized (likely by the incoming oxygen) and recrystallized into pores. The formation of new phases during treatment at high temperature (1400 °C) was verified. In the XRD pattern of a superficial layer (4 mm from the external surface) of B without superficial conditioning (NC) treated at 1400 °C for 5 h, peaks assigned to magnesia-alumina spinel (File N° 82-2424) together with other low-intensity peaks of SiO_2 (File N° 87-2096) and SiC (File N° 73-1662) where identified as new crystalline phases. The presence of MgO-Al_2O_3 spinel has also been verified by cathodoluminescence [29] in specimens of A1, A2, and B treated under similar thermal and atmospheric conditions. Despite no certain evidence of a superficial and continuous dense MgO layer being detected in any of the specimens tested at 1400 °C, the presence of MgO (identified by SEM/EDS) as white solid spots around magnesia aggregates on the external surface specimens without surface conditioning was observed in B after 5 h (Fig. 7). This fact is considered as indicative of the presence of gaseous magnesium at least, which reacts later with the atmospheric O_2 to form MgO outside the specimen.

At 1400 °C, material B exhibited the best resistance to gas attack by air measured by mass loss and decarburized area in any of the time periods and for any surface conditioning. This fact was mainly attributed to the higher content of antioxidant additives together with the combination of Al-Mg and Si which result in a better protection against graphite oxidation covering a broad range of temperature [30, 31]. Apparently, the global open porosity (Fig. 4) did not determine the chemical resistance of the specimens. Conversely, comparing the chemical wear of NC, P and M specimens, it was evident that only the muffle with graphite is a suitable strategy to increase material resistance to air attack to a significant extent.

In NC and P specimens after 5 h at 1400 °C, an intermediate area with an intermediate darkness between the external decarburized zone and the dark central area was detected, as is shown in Fig. 8; these zones were called "semidecarburized areas" (SD). This particular feature was not previously reported in the literature for MgO-C refractories. The semidecarburization phenomenon is explained considering the simultaneous occurrence of both, the direct (I) and indirect (II) oxidation of graphite. At 1400 °C, the carbothermal reduction reaction (II) could occur if the thermodynamic conditions are fulfilled [26, 32]. Besides others variables, this reaction is dependent on the partial pressure of the gases such as Mg, CO, and O_2. Low partial pressures of these gases (<<1 atm) favor the occurrence of reaction (II) to the right [1, 7, 26, 32]. Moreover, the rate of this solid-solid reaction is mainly limited by chemical reaction in the initial stage and by the diffusion of product gases to the surface in the final stage [7]. Conversely, a gradient of oxygen partial pressure is generated within the specimen when the thermal treatment progresses primarily due to the effect of both thermal and porosity gradients. Thus, the carbothermal reduction is more favored in the center of the specimen where the amount of O_2 is low and it is less favored in the outer layer where the partial pressure is higher. Simultaneously, the direct oxidation of graphite preferentially occurs in the outer layers of the specimen; this reaction is controlled by O_2 diffusion [1, 2, 4, 10, 13, 14, 16]. If the direct oxidation (I) is the main source of CO (g), the negative gradient of concentration of this gas toward the center of the specimen has the same effect as the gradient of O_2 concentration on reaction (II). Thus, the SD area generates in the region of the specimen where both reactions, the carbothermal reduction and the oxidation of graphite, are competitive; the presence of these regions are even favored by the effect of the opposite flow of gaseous reaction products such as Mg and CO by reaction (II). Conversely, the lower amount of graphite in the outer layers of the specimen lost by reaction (I) contributes to accentuating the gradient of the advance of the carbothermal reduction between the center and the superficial layers of the specimen.

This explanation for the formation of the SD zone is supported by the change of the size of magnesia particles determined by image analysis. After 5 h at 1400 °C, a signif-

icant reduction of the magnesia aggregates' size in NC specimens was determined which was attributed to the consumption of this phase by metallic vaporization and metallothermic or carbothermal reduction. However, differences where observed between the change in the size of inner and outer particles. For pitch-bonded materials, reductions around 35 % and 20 % were measured for inner and outer MgO particles, respectively; for the resin-bonded refractory, the inner particles reduced 45 % and the outer particles reduced 25 %. These facts indicate that the process leading to the consumption of magnesia (which produce gaseous Mg) is more favored in the center of the specimen where the particle size reduction is more pronounced; for this reason, the carbothermal reduction is the main candidate to produce this differential change of the particle size based on the strong dependence of this reaction on O_2 partial pressure and graphite content. The other reactions producing gaseous magnesium could, of course, also occur. In regard to the difference between both types of refractories, the MgO particles became smaller in the inner region of B specimens where carbothermal reduction would prevail; this coincides with the fact that B is a unique material in which the presence of recrystallized magnesia was confirmed on the specimen's surface. It is worth noting that the formation of a dense MgO layer (which was not certainly verified in any of the tested specimens) is neither a requirement nor the sole indicator of the occurrence of the reaction between MgO and C.

On the basis of the above explanation, when the O_2 gradient is developed but the carbothermal reaction does not occur it is expected that the oxidation of graphite would produce a clear reaction front. This is the case for the thermal treatments of NC and P specimens at 660 °C (3 h and 5 h). Conversely, until the gradient of the oxygen partial pressure is well established at conditions where carbothermal reduction is able to occur, no SD is observed and a clear reaction front for direct oxidation (I) is developed as occurs in thermal treatments at 1400 °C for 3 h.

4 Conclusions

Thermochemical degradation in three commercial resin- and pitch-bonded MgO-C refractories subjected to the attack of atmospheric air over a wide range of temperatures was evaluated by mass loss determination and decarburized area measurements. The main conclusions are the following:

- At 660 °C, the chemical degradation was higher in the resin-based refractory, in spite of its lower content of organic binder; at this temperature: the organic binders carbonize, the residual carbon oxidizes, open porosity increases, and graphite oxidation is just begun. A severe microstructural degradation with a radial advance was observed.
- When heating up to 1400 °C, the main aggressive process is direct graphite oxidation. Several transformations occur up to this temperature, including both chemical reactions and porosity modifications. In this case, the oxidation resistance is found to be strongly affected by the different metallic additives (Mg-Al, Al and Si powders).
- At 1400 °C, an intermediate region between the dark core and the completely decarburized outer layer is found in most of the samples. This so-called "semidecarburized area" is attributed to a competition between two different graphite oxidation processes: direct and indirect oxidation of graphite (or carbothermal reduction).
- In terms of specimen surface conditioning, only those muffled with graphite powder were shown to be really protective against the chemical attack of air at 1400 °C and can be considered to minimize oxidation in laboratory tests.

Finally, it is important to emphasize that the experimental data obtained in this study and the interpretation in terms of mechanisms and microstructural changes represent valuable information that can be used directly by users, since these refractories have been used in Tenaris steelshops as working lining materials in both electric arc furnaces and ladles.

References

[1] **Li, X., Rigaud, M., Palco, S.:** J. Amer. Ceram. Soc. **78** (1995) [4] 965–971
[2] **Ghosh, N.K., Ghosh, D.N., Jagannathan, K.P.:** Brit. Ceram. Trans. **99** (2000) [3] 124–128
[3] **Sadrnezhaad, S.K., Mahshid, S., Hasemi, B., Nemati, Z.A.:** J. Amer. Ceram. Soc. **89** (2006) [4] 1308–1316
[4] **Baker, B.H., Brezny, B.:** Proceedings of UNITECR'91, Aachen, Germany (1991) 168–172
[5] **Yamaguchi, A.:** Fundamentals of Refractory Technology, Ceramic Transactions (Vol 125), Edited by J. Bennett and J.D. Smith. The American Ceramic Society, Westerville (2001) 157–170
[6] **Baudín, C.:** Fundamentals of Refractory Technology, Ceramic Transactions (Vol.125), Edited by J. Bennett and J.D. Smith. The American Ceramic Society, Westerville (2001) 73–92
[7] **Tabata, K., Nishio, H., Itoh, K.:** Taikabutsu Overseas **8** (1988) [4] 3–10
[8] **Rigaud, M., Bombard, P., Li, X., Guéroult, B.:** Proceedings of the UNITECR'93, São Paulo, Brazil (1993) 360–371
[9] **Kanno, K., Koike, N., Korai, Y., Mochida, I., Komatsu**, M.: Carbon **37** (1999) 195–201
[10] **Faghihi-Sani, M., Yamaguchi, A.:** Ceram. Internat. **28** (2002) 835–839
[11] **Quintela, M.A., Pessoa, C.A., Rodrigues, J.A., Pandolfelli, V.C.:** Refractories Application & News (2002) [January/ February] 16–19
[12] **Takeuchi, K., Yoshida, S., Tsuboi, S.:** J. Tech. Assoc. Refr. Japan **23** (2003) [4] 276–279
[13] **Sunayama, H., Kawahara, M.:** J. Tech. Assoc. Refr. Japan, **23** (2003) [3] 152–155
[14] **Hashemi, B., Nemati, Z.A., Faghihi-Sani, M.A.:** Ceram. Internat. **32** (2006) 313–319
[15] **Quintela, M.A., Santos, F.D., Pessoa, C.A., Rodriguez, J. de A., Pandolfelli, V.C.:** Refractories Application and News (2006) [September/ October] 15–19
[16] **Sadrnezhaad, K., Nemati, Z.A., Mahshid, S., Hosseini, S., Hasehmi, B.:** J. Amer. Ceram. Soc. **90** (2007) [2] 509–515
[17] **Gokce, A.S., Gurcan, C., Ozgen, S., Aysin, S.:** Ceram. Internat. **34** (2008) 323–330
[18] DIN EN 993-1. Method of test for dense shaped refractory products. Determination of bulk density, apparent porosity and true porosity. (DIN 51056), (1995)
[19] ASTM 329-88. Standard test method for specific gravity of fired ceramic whiteware materials, (1994)
[20] **Muñoz, V., Rohr, G.A., Cavalieri, A.L., Tomba Martinez, A.G.:** J. Test. Eval. **40** (2012) 1
[21] **Rand, B., McEnaney, B.:** Brit. Ceram. Trans. J. **84** (1985) 175–165
[22] **Taffin, C., Poirier, J.:** Interceram **43** (1994) [5] 354–358 / [6] 458–460
[23] **Bavand-Vandchali, M., Golestani-Fard, F., Sarpoolaky, H., Rezai, H.R., Aneziris, C.G.:** J. Europ. Ceram. Soc. **28** (2008) 563–569
[24] **Vieira, W., Rand, B.:** Proceedings UNITECR'97, New Orleans, USA (1997) 851–859
[25] **Gardziella, A., Suren, J., Belsue, M.:** Interceram **41** (1992) [7/8] 461–467
[26] **Baudín, C., Alvarez, C., Moore, R.:** J. Amer. Ceram. Soc. **82** (1999) [1] 3529–3538
[27] **Baudson, H., Debucquoy, F., Huger, M., Gault, C., Rigaud**, M.: J. Europ. Ceram. Soc. **19** (1999) 1895–1901
[28] **Brant, P.O.R.C., Rand, B.:** Proceedings of UNITECR'91, Aachen, Germany (1991)
[29] **Cavalieri, AL., Tomba Martinez, A.G., Karakus**, M.: Proceedings of SAM-CONAMET (CD-ROM), Santiago, Chile (2006)
[30] **Nandy, S.K., Ghosh, N.K., Das, G.C.:** Proceedings of UNITECR'05, Orlando, USA (2005)
[31] **Hanagiri, S., Harada, T., Aso, S., Fujihara, S., Yasui, H., Takanaga, S., Takahashi, H., Watanabe, A.:** Taikabutsu Overseas **13** (1993) [3] 20–21
[32] **Baudín, C., Alvarez, C.:** Proceedings of UNITECR'95, Kyoto, Japan (1995) 108–115

Received: 25.04.2012